



ARTICLE

Combined Effects of GrowGx™ and Collagen Peptide on UVB-Induced Skin Aging: An In Vitro and In Vivo Analysis

Zhijia Lu^{1,2,3*}, Xi Lu^{1,2,3*}, Meng Liu^{2,3,4}, Xiaoqun Duan^{2,3,4}¹School of Pharmacy, Guilin Medical University, Guilin, Guangxi Province 541199, China²School of Biomedical and Pharmaceutical Sciences, Guilin Medical University, Guilin, Guangxi Province 541199, China³Industrial Technology Research Institute, Guilin Medical University, Guilin, Guangxi Province 541199, China⁴School of Pharmacy, Macau University of Science and Technology, Macau, 999078, China

*co-first authors

ARTICLE INFO

Received 18 October 2023

Accepted 2 November 2023

Online 26 November 2023

KEY WORDS:

Ultraviolet B (UVB);

Photoaging;

GrowGx™;

Collagen Peptide;

Anti-aging

Abstract

This study aims to assess the anti-aging effects of GrowGx™ combined with Collagen Peptide (CP) on human keratinocyte (HaCaT) cells and mice exposed to Ultraviolet B (UVB) radiation. An in vitro model using UVB-induced HaCaT cells was developed to examine the impact of GrowGx™ and CP on cell viability, oxidative stress markers, and cellular damage repair mechanisms. Simultaneously, an in vivo mouse model was established to evaluate the compound's safety profile and its efficacy against UVB-induced skin aging. The experimental groups included a Normal Control (NC), a UVB-exposed group, GrowGx™ group, CP group, a combination group of GrowGx™ and CP (GrowGx™ + CP), and a Vitamin C (VC) positive control group. The in vitro results demonstrated a significant decline in cell viability and an increase in SA-β-gal content post-UVB exposure in the UVB group. Additionally, there was a disruption in cellular oxidative balance, indicated by elevated MDA levels and decreased SOD and HYP concentrations. Treatment with GrowGx™ and CP, individually or in combination, led to a restoration of cell viability, reduced SA-β-gal content, and reestablished oxidative equilibrium. The scratch assay further confirmed the enhancement in HaCaT cell proliferative capacity following GrowGx™ and CP treatment. In vivo findings revealed pronounced skin wrinkles, dryness, and reduced elasticity in UVB-exposed mice, which were ameliorated upon treatment with GrowGx™, CP, or their combination, with the latter showing the most significant improvement. The study concludes that the synergistic application of GrowGx™ and CP exhibits a more pronounced anti-aging effect on UVB-induced skin aging in mice, potentially through mechanisms involving enhanced cell proliferation and reduced oxidative stress.

Corresponding author: Xiaoqun Duan, School of Biomedical and Pharmaceutical Sciences, Guilin Medical University, Guilin, Guangxi, 541199, China; Industrial Technology Research Institute, Guilin Medical University, Guilin, Guangxi, 541199, China; School of Pharmacy, Macau University of Science and Technology, Macau, 999078, China. 2569589268@qq.com

Introduction

The skin, as the human body's most extensive and outermost organ, serves as a critical barrier, shielding the body from a variety of stimuli including physical, chemical, and infectious agents (Lopez-Otin et al., 2023). Comprising the epidermal, dermal, and subcutaneous layers, the dermis is primarily made up of collagen and elastic fibers. Collagen, a key component of the dermis, is a linear protein that provides structural support and strength, crucial for maintaining skin elasticity and firmness. Similar to other body organs, the skin is subject to aging, influenced by metabolic, endocrine, and genetic factors. Notably, ultraviolet (UV) exposure accelerates skin aging more significantly compared to other organs (Im et al., 2019).

Photoaging, a term for aging induced by prolonged UV exposure, initially presents as erythema formation and reduced skin hydration (Im et al., 2019). Over time, prolonged UV exposure leads to an accumulation of Reactive Oxygen Species (ROS) (Bang et al., 2021), resulting in collagen degradation, wrinkle formation, and potentially leading to lentigines, acne, and even skin cancer. ROS activates the mitogen-activated protein kinase (MAPK) family, further triggering the p38, JNK, and ERK signalling pathways. This activation ultimately induces the expression of matrix metalloproteinases (MMPs), enzymes responsible for degrading collagen, proteoglycans, and other matrix proteins, thereby contributing to skin aging (Subedi et al., 2017; Han et al., 2019; Choi et al., 2021; Mu et al., 2021). Among UV rays (UVA, UVB, UVC), UVB is characterized by shorter wavelengths and higher energy. It predominantly accumulates in the epidermis, causing epidermal hyperproliferation, wrinkles, and reduced elasticity - key features of photoaging (Chen et al., 2020). Remarkably, UVB's skin damage potential is 800-1000 times greater than UVA at equivalent dosages (Gilchrest et al., 1996) and is also known to induce DNA damage, leading to keratinocyte death (Vats et al., 2021). Consequently, UVB was chosen as the experimental light source for this study. HaCaT cells, located in the basal layer of the skin and known for their defensive functions, low differentiation, and high proliferative capacity (Yue et al., 2022), were selected for their ease of culture and genetic stability, making them an optimal model for studying skin photoaging.

GrowGx™, developed by Guilin Guxin Biotechnology Co., Ltd., is a yeast fermentation-derived small molecule with demonstrated efficacy in promoting repair of damaged cells. Preliminary research by our team revealed that at a concentration of 5 mg/mL, GrowGx™ enhances fibroblast repair processes and improves skin texture, reducing spots and pores, and rendering the skin smoother (Zhang et al., 2022). Oral collagen supplementation, a growing trend in the anti-aging sector, has been shown to enhance skin hydration,

elasticity, and dermal collagen density (Bolke et al., 2019). A 12-week clinical trial highlighted the benefits of orally supplemented low molecular weight collagen peptides in enhancing human skin elasticity and reducing wrinkles (Kim et al., 2022). However, it was also noted that the bioavailability of orally supplemented collagen peptides in rats is less than 60% (Wang et al., 2015). The collagen peptides (CP) used in our laboratory were self-prepared, filtered through dextran gel, and characterized by a molecular weight below 700 kDa.

Current cosmetic formulations often incorporate multiple active ingredients to exert synergistic anti-aging effects. In this context, our study aims to evaluate the efficacy of GrowGx™ in combination with CP against skin photoaging through the development of both in vitro and in vivo anti-aging models. The results of our experiments indicate that the combined application of GrowGx™ and CP offers more substantial anti-photoaging benefits compared to their individual use.

Materials and Methods

1. Materials

Collagen peptides were extracted from fish in our laboratory. GrowGx™ was obtained from Guilin Guxin Biotechnology Co., Ltd. Assay kits for SOD (Solarbio, Cat# BC0170), hydroxyproline (HYP) (Solarbio, Cat# BC0250), malondialdehyde (MDA) (Nanjing Jiancheng, Cat# A003-1-2), and β -galactosidase (β -GAL) (Nanjing Jiancheng, Cat# H578) were utilized. Antibodies for MMP-1 (1:1000, abcam, Cat# ab134184), MMP-9 (1:1000, abcam, Cat# ab76003), Collagen- I (1:1000, affinity, Cat# AF7001), p21 (1:1000, affinity, Cat# DF6423), TGF- β (1:2000, proteintech, Cat# 21898-1-AP), and GAPDH (1:10000, abcam, Cat# ab8245) were used. UVB-310 lamps and a UVB radiometer were supplied by Nanjing Kazi Electronic Co., Ltd. An UV intensity meter was provided by Suzhou Keyinuo Precision Photoelectricity Co., Ltd. An inverted microscope was obtained from Guangzhou Mingmei Optoelectronic Technology Co., Ltd.

2. Cell Culture

Human immortalized keratinocytes (HaCaT cells) were acquired from Guangzhou Saiku Biotechnology Co., Ltd. (Item No.: CC4013) and cultured at 37°C in a 5% CO₂ incubator. Cells were maintained in DMEM (Solarbio, Cat# 11995) supplemented with 10% FBS. At 80–90% confluency, cells were passaged using 0.25% trypsin-EDTA solution without phenol red (Solarbio Cat# 11995).

For the UV-induced HaCaT photoaging model, cell suspensions (2×10^4 cells/mL) were seeded in 96-well plates (150 μ l/well) and incubated for 12 hours to allow attachment. After removal of the supernatant, cells were starved for 12 hours in serum-free DMEM before UV irradiation (UV doses:

0, 10, 25, 50, 75, 100 mJ/cm²). Cells were washed with PBS thrice to avoid medium absorption of UV and then covered with PBS during irradiation. Post-24-hour irradiation, 20 µL of MTT (5 mg/mL) was added to each well and incubated for 4 hours. The liquid was aspirated from the wells, and 200 µL of DMSO was added to dissolve the formazan crystals. Absorbance was measured at 490 nm using a microplate reader to calculate cell viability.

Cell proliferation was assessed using varying concentrations of GrowGx™ (10, 30, 60, 90 µg/ml) and CP (10, 20, 40, 80 µg/ml) and their 16 possible combinations for 24 hours, followed by MTT assay.

For determining the survival rate of photoaged HaCaT cells treated with GrowGx™ combined with CP, post-UV irradiated cells were treated with the optimized concentrations of GrowGx™ and CP for an additional 24 hours before MTT assay.

3. Scratch Assay

HaCaT cells were cultured in 6-well plates until 95% confluency. After aspiration of the medium, a straight scratch was made using a 200 µL pipette tip. Cells were washed with PBS to remove debris and incubated in medium containing GrowGx™ and CP. Wound closure was photographed at 0 and 24 hours using an inverted microscope, and the area of closure was calculated.

4. SA-β-gal Assay

HaCaT cells were seeded in 6-well plates and allowed to attach. After washing thrice with PBS and UV irradiation, cells were treated with the drugs for 24 hours. The SA-β-gal assay was performed according to the kit's instructions with a 12-hour water bath incubation. Five random fields were chosen for counting positive cells.

5. Animal Grouping and Treatment

Specific Pathogen-Free (SPF) female Kunming mice (6 weeks old, 18–22 g) were sourced from Hunan Slaccas Jinda Experimental Animal Co., Ltd. They were acclimatized for a week under standard conditions with free access to standard feed and water.

The acclimatized mice were randomly divided into six groups: Normal Control (NC), Model (UVB), Positive Control

(VC), Yeast Fermentate (GrowGx™), Collagen Peptide (CP), and Yeast Fermentate combined with Collagen Peptide (GrowGx™ + CP), with 6 mice per group (n = 6). Hair was removed from a 3 cm × 3 cm area on their backs using depilatory cream. The experimental groups were treated as specified in the subsequent table.

The photoaging model for aged mice was developed in accordance with methodologies described in previous literature (Tian et al., 2021) and findings from our preliminary research. The established Minimum Erythema Dose (MED) for mouse skin post-ultraviolet (UV) irradiation was identified as 150 mJ/cm².

For drug administration, as outlined in Table 1, UV irradiation was conducted 2 hours post-administration. Except for the normal control group, which did not undergo UV exposure, the remaining five treatment groups received an initial daily dose of one MED of UV radiation for the first week. This dose was incrementally increased by one MED each week. From the fifth week onwards, the regimen consisted of a consistent daily dose of four MEDs until the conclusion of the experiment in the sixth week.

All experimental procedures involving animals were approved by the Animal Ethics Committee of Guilin Medical College, approval number GLMC202103003. The experiments were carried out in strict adherence to the animal care and use guidelines of Guilin Medical College.

6. In Vivo Safety Assessment

The safety of the tested compounds in vivo was assessed via body weight and organ indices of the mice (Cao et al., 2022). The body weight of the Kunming mice was monitored on a weekly basis. At the conclusion of the experiment, the mice were euthanized, and blood samples were collected. The dorsal skin, liver, kidney, thymus, and spleen were rapidly dissected on ice, cleared of connective tissue, patted dry, and weighed. The organ index for each tissue was calculated using the formula:

$$\text{Organ Index (mg/g)} = \text{Organ Weight (mg)} / \text{Mouse Body Weight (g)}$$

7. Macroscopic Evaluation of Mouse Skin

Throughout the experimental period, the dorsal skin of the mice was evaluated and scored weekly for photoaging characteristics

Table 1. Animal grouping and administration treatment

Groups	Experimental Condition	Treatment Description	Drug Concentration (mg/mL)
NC	NO UVB irradiation	NO treatment	0
UVB	UVB irradiation	Ultrapure water	0
VC	UVB irradiation	VC	10
GrowGx™	UVB irradiation	GrowGx™	4
CP	UVB irradiation	CP	8
GrowGx™ + CP	UVB irradiation	GrowGx™ + CP	4 + 8

based on criteria established in reference (Cicek et al., 2021). Photographs documenting the condition of the dorsal skin were taken for macroscopic assessment, as detailed in Table 2.

8. Skin Elasticity Recovery Time

Modifying the methods described in literature (Song et al., 2017), the dorsal skin of the mice was gently lifted along the midline. The time taken for the skin to return to its original state was measured from the moment the mice's limbs were lifted off the ground.

9. Skin Morphology and Structure Analysis

Dorsal skin samples from mice were fixed, subjected to ethanol dehydration, embedded, and then stained using Hematoxylin and Eosin (H&E) and Masson's trichrome. Changes in the skin structure post-UV irradiation were observed under a microscope.

10. Antioxidant Marker Analysis

Levels of malondialdehyde (MDA), superoxide dismutase (SOD), and hydroxyproline (HYP) in mouse skin and HaCaT cells were determined using the respective assay kits.

11. Western Blot Analysis

Samples stored at -80°C were lysed in RIPA buffer and centrifuged (12,000 rpm, 4°C , 15 min). The supernatant was collected for protein quantification using the BCA assay. The samples were then subjected to 10% SDS-PAGE (80 V for 30 min, 120 V for 1 h) and transferred to PVDF membranes. The transfer conditions were set at 220 mA for 120 min. Membranes were blocked in 5% skim milk at room temperature for 2 hours, followed by overnight incubation with primary antibodies at 4°C and 2 hours with secondary antibodies at room temperature.

12. Statistical Analysis

Data were analysed using GraphPad Prism 9.0 (GraphPad Software, Inc., La Jolla, CA, USA) and presented as mean \pm standard error of the mean (SEM) from at least three independent experiments. One-way ANOVA followed by Tukey's post hoc test was employed for statistical evaluation. A P -value < 0.05 was considered statistically significant.

Table 2. The grading scale for evaluation of photoaging

Grade	Evaluation criteria
0	No wrinkles or laxity; fine striations running the length of the body
1	Fine striations
2	The disappearance of all fine striations
3	Shallow wrinkles
4	A few deep wrinkles and laxity
5	Increased deep wrinkles
6	Severe wrinkles; development of tumors/lesions

Results

1. Assessment of Cell Viability

The UV irradiation dose had a significant effect on HaCaT cell viability, with a marked reduction observed as the dose increased ($P < 0.05$). At a dose of 50 mJ/cm^2 , the cell survival rate was recorded at $60.97 \pm 6.8\%$. Increasing the dose to 75 mJ/cm^2 further decreased the survival rate to $36.5 \pm 11.7\%$ (Figure 1A). In light of these findings, a dose of 50 mJ/cm^2 was selected for subsequent experiments (Zhang et al., 2022).

An increase in GrowGx™ concentration to $90 \text{ }\mu\text{g/mL}$ significantly enhanced HaCaT cell proliferation ($P < 0.05$). However, CP at the doses tested ($10, 20, 40, 80 \text{ }\mu\text{g/mL}$) did not show a significant effect on cell proliferation. The study revealed that specific combinations of CP ($80 \text{ }\mu\text{g/mL}$) with GrowGx™ ($60 \text{ }\mu\text{g/mL}$), CP ($40 \text{ }\mu\text{g/mL}$) with GrowGx™ ($90 \text{ }\mu\text{g/mL}$), and CP ($80 \text{ }\mu\text{g/mL}$) with GrowGx™ ($90 \text{ }\mu\text{g/mL}$) significantly promoted HaCaT cell proliferation (Figure 1B).

Post-UVB irradiation, a notable decrease in the survival rate of HaCaT cells was observed ($P < 0.01$). However, the combination of CP ($40 \text{ }\mu\text{g/mL}$) with GrowGx™ ($90 \text{ }\mu\text{g/mL}$) significantly improved the survival rate of HaCaT cells (Figure 1C). This suggests that the combination of GrowGx™ ($90 \text{ }\mu\text{g/mL}$) and CP ($40 \text{ }\mu\text{g/mL}$) effectively mitigates UVB-induced damage in HaCaT cells, a capability not observed with either GrowGx™ ($90 \text{ }\mu\text{g/mL}$) or CP ($40 \text{ }\mu\text{g/mL}$) alone.

2. HaCaT Cell Scratch Assay

Cellular aging is often characterized by diminished proliferative and division capabilities, leading to prolonged wound healing times (Lopez-Otin et al., 2012; Lopez-Otin et al., 2023). Thus, enhancing cell proliferation is considered a viable anti-aging strategy. At 24 hours post-treatment (Figure 2), a significant reduction in the wound healing area was observed in the GrowGx™ group, GrowGx™ combined with CP group, and the VC group ($P < 0.01$). However, no significant decrease in wound healing area was noted in the CP group ($P > 0.05$). These findings suggest that both GrowGx™ and its combination with CP exhibit anti-aging potential, with the combination retaining the proliferative properties of GrowGx™.

3. Measurement of SA- β -gal Content in HaCaT Cells

UVB irradiation led to an increase in lysosomal content and SA- β -gal activity, thereby triggering the activation of p16 protein and related signaling pathways, culminating in cellular senescence (Jiang et al., 2022). Thus, SA- β -gal activity serves as a marker to reflect the anti-aging efficacy of GrowGx™ combined with CP. Upon analysis under a microscope, a significant elevation in SA- β -gal content was observed in the UVB group ($P < 0.01$), indicating successful

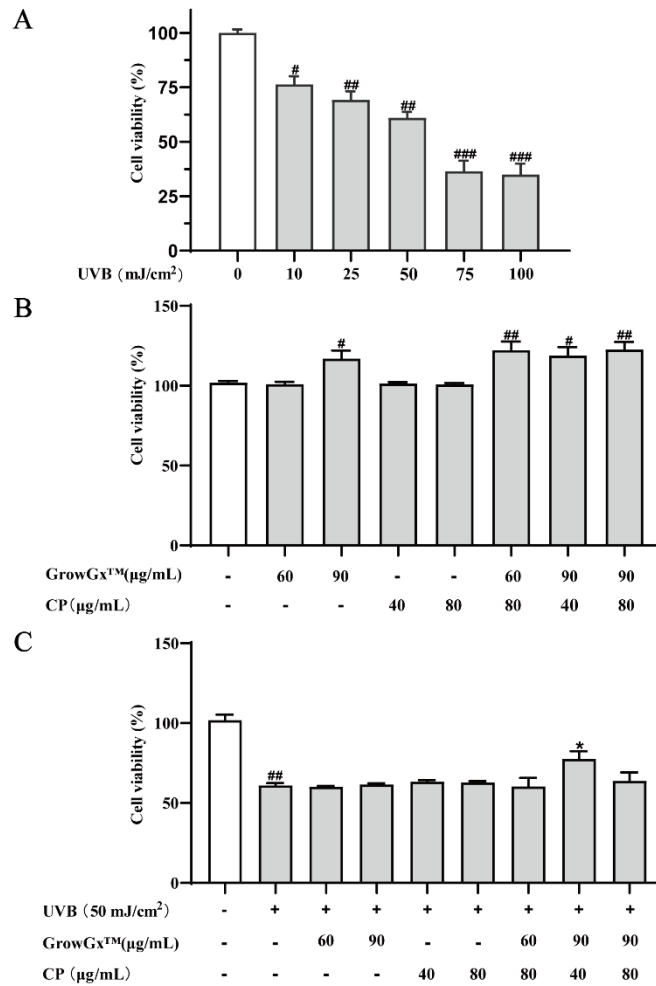


Figure 1. Cell viability assessment in HaCaT cells

(A) illustrates the impact of varying UV irradiation doses on HaCaT cell viability. (B) demonstrates the effect of the combined treatment of GrowGx™ and Collagen Peptide (CP) on the proliferation of HaCaT cells. (C) details the influence of GrowGx™ and CP on the survival rate of photoaged HaCaT cells. Each bar graph represents the mean ± Standard Error of the Mean (SEM) based on six replicates (n = 6). Notably, statistical significance was observed in comparison to the Normal Control (NC) group (^{###}*P* < 0.001, ^{##}*P* < 0.01, [#]*P* < 0.05) and the UVB group (^{###}*P* < 0.001, ^{**}*P* < 0.01, ^{*}*P* < 0.05).

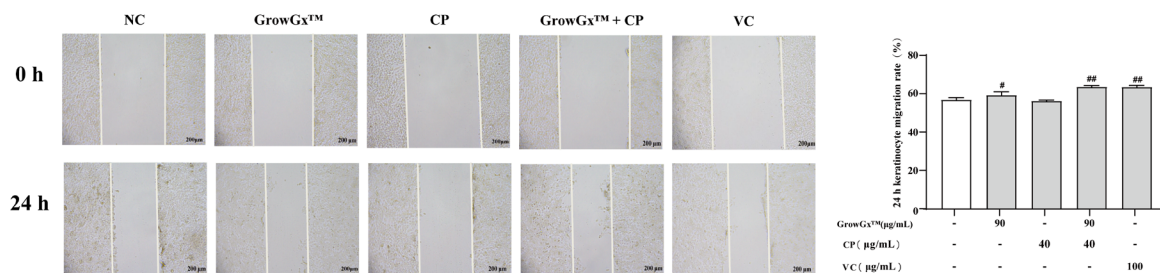


Figure 2. The effects of the combined application of GrowGx™ and CP on the repair of damaged HaCaT cells in a scratch assay

Each bar graph represents the mean ± SEM for three replicates (n = 3). The results indicated statistical significance in comparison to both the NC group (^{###}*P* < 0.001, ^{##}*P* < 0.01, [#]*P* < 0.05) and the UVB group (^{###}*P* < 0.001, ^{**}*P* < 0.01, ^{*}*P* < 0.05).

model establishment (Figure 3). The combined treatment of GrowGx™ and CP significantly reduced SA-β-gal content in HaCaT cells (*P* < 0.05), suggesting a higher physiological activity compared to GrowGx™ or CP alone and an ability to inhibit UV-induced SA-β-gal release in HaCaT cells.

4. Measurement of MDA, SOD, and HYP in Cells

MDA and SOD are oxidative balance markers, while HYP is a primary component of collagen, making them crucial

indicators for assessing aging. The UVB group showed a significant decrease in SOD and HYP levels (*P* < 0.01) and an increase in MDA levels (*P* < 0.01), indicating a disruption in cellular oxidative balance and aging (Figure 4). The CP group demonstrated a significant increase in cellular HYP content (*P* < 0.05), while MDA and SOD levels showed no significant difference, indicating that CP can supplement HYP content. The combination of GrowGx™ and CP significantly increased SOD and HYP levels (*P* < 0.05) and decreased MDA levels (*P* <

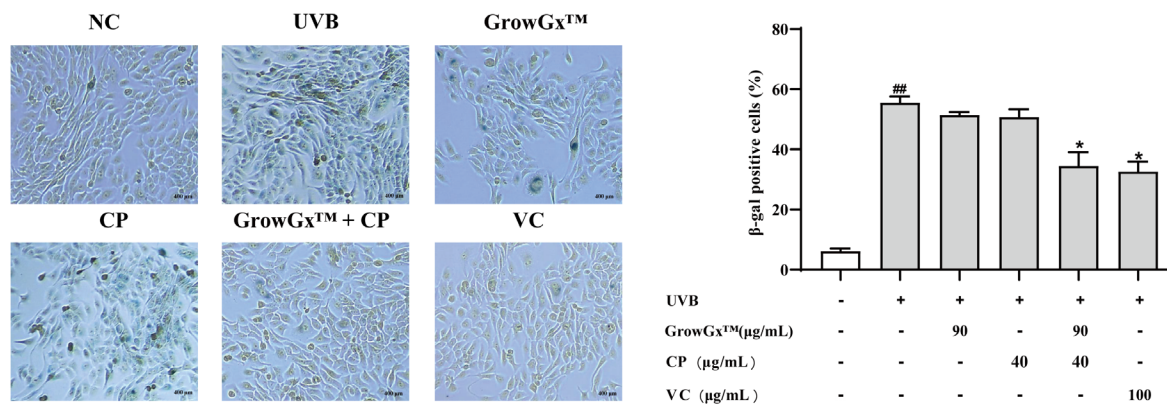


Figure 3. Analysis of SA-β-gal content in HaCaT cells

The study evaluated the impact of GrowGx™ combined with Collagen Peptide (CP) on SA-β-gal levels in photoaged HaCaT cells. Each bar graph represents the mean ± Standard Error of the Mean (SEM) for three replicates (n = 3). Statistical significance was noted in comparison to both the Normal Control (NC) group (^{###}*P* < 0.001, ^{##}*P* < 0.01, [#]*P* < 0.05) and the UVB group (^{***}*P* < 0.001, ^{**}*P* < 0.01, ^{*}*P* < 0.05).

0.01), suggesting that this combination can reduce oxidative levels, enhance antioxidant capacity, and promote collagen synthesis, thereby achieving anti-aging effects.

5. Measurement of p21, MMP-1, MMP-9, Collagen I, TGF-β in Cells

In the UVB group, increased p21 expression (*P* < 0.01) indicated successful aging model establishment, while a decrease in TGF-β expression (*P* < 0.01) was observed, suggesting a correlation between cellular aging and TGF-β levels (Figure 5A). Compared to the UVB group, the CP group exhibited a decrease in p21 expression (*P* < 0.05), while TGF-β expression showed no significant difference. In the GrowGx™ group, TGF-β expression increased (*P* < 0.05), with no significant difference in p21 expression. The combination of GrowGx™ and CP led to a decrease in p21 expression (*P* < 0.01) and an increase in TGF-β expression (*P* < 0.01), indicating that this combination can activate TGF-β while inhibiting p21 expression, thereby exerting anti-aging effects (Figure 5A).

The UVB group exhibited a significant increase in MMP-1 and MMP-9 expression (*P* < 0.01) and a decrease in Collagen I expression (*P* < 0.01), indicative of collagen degradation post-UV irradiation. The CP group showed an increase in Collagen I expression (*P* < 0.05) and a decrease in MMP-1 expression (*P* < 0.05). The GrowGx™ group did not show any significant difference in Collagen I and MMP-1 expression. However, the combination of GrowGx™ and CP significantly reduced MMP-1 (*P* < 0.01) and MMP-9 (*P* < 0.05) expression and increased Collagen I expression (*P* < 0.01), suggesting that this combination can alleviate UVB-induced collagen degradation in HaCaT cells (Figure 5B).

6. In Vivo Safety Assessment of GrowGx™ Combined with CP

The preliminary assessment of the toxicological effects of

the test compounds on the test animals was conducted by measuring changes in body weight and organ indices (Zhang et al., 2010). This study monitored the body weight of the mice and measured the weights of the liver, spleen, and thymus at the end of the experiment to calculate their organ indices. The results, presented in Tables 3 and 4, indicate no significant differences in body weight changes and organ indices among the NC, UVB, and treatment groups (*P* > 0.05). This suggests that at the tested doses, UV irradiation and drug treatments did not exhibit noticeable toxicological effects on the mice.

7. Macroscopic Evaluation of Mouse Skin

In alignment with references (Song et al., 2018; Zhang et al., 2020), female Kunming mice were selected as the animal model for anti-aging research. As observed in Figure 6C, the UVB group exhibited photoaging characteristics in the skin such as wrinkles, pigmentation, dryness, laxity, and reduced elasticity. The visual scores significantly increased (*P* < 0.01), and the elasticity recovery time was substantially extended (*P* < 0.01), consistent with previously reported photoaging phenomena (Battie et al., 2014), confirming the successful establishment of the photoaging model. The CP group showed a decrease in visual scores (*P* < 0.05) and a reduction in elasticity recovery time (*P* < 0.05). In the group treated with GrowGx™ combined with CP, there was a noticeable decrease in skin wrinkles, improved skin fullness and elasticity, reduced visual scores (*P* < 0.01), and shortened elasticity recovery time (*P* < 0.01), indicating the effectiveness of GrowGx™ combined with CP in alleviating UV-induced photoaging in mouse skin.

8. Effect of GrowGx™ Combined with CP on MDA, SOD, and HYP Levels in Mouse Skin

As depicted in Figure 6F, the UVB group showed a decrease in SOD and HYP levels (*P* < 0.01) and an increase in MDA

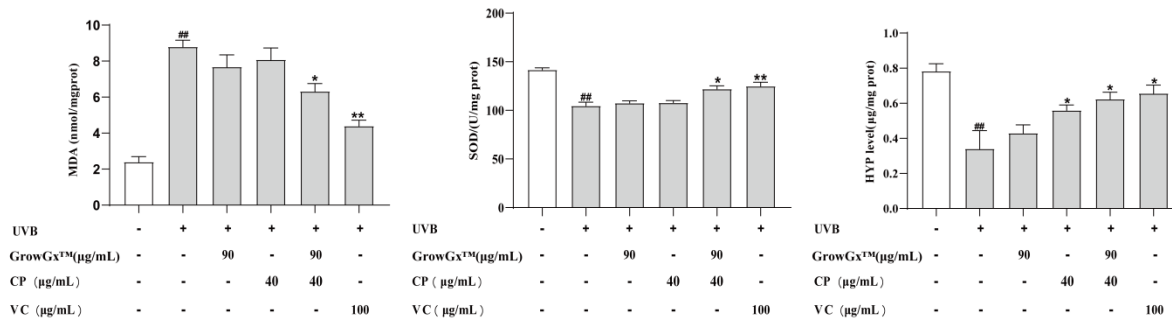


Figure 4. Analysis of MDA, SOD, and HYP levels in HaCaT cells

The study assessed the effects of GrowGx™ combined with CP on MDA, SOD, and HYP levels in photoaged HaCaT cells. Each bar graph represents the mean ± SEM for three replicates (n = 3). Statistical significance was established in comparison to the NC group (###*P* < 0.001, ##*P* < 0.01, #*P* < 0.05) and the UVB group (****P* < 0.001, ***P* < 0.01, **P* < 0.05).

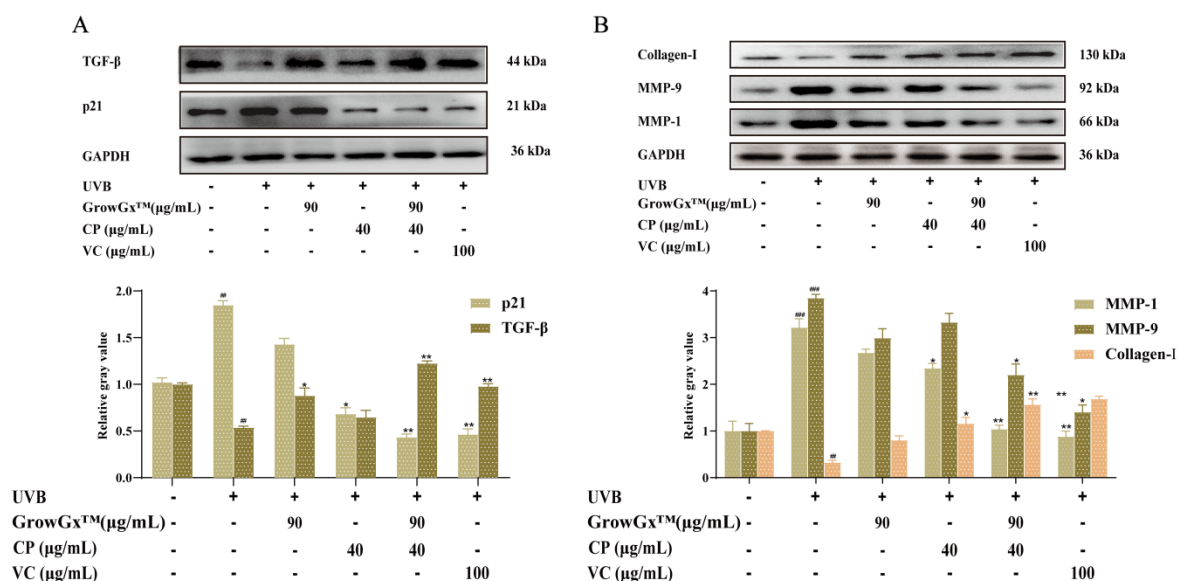


Figure 5. Levels of p21, MMP-1, MMP-9, Collagen I, TGF-β in HaCaT cells

(A) Expression of p21 and TGF-β proteins. (B) Expression of MMP-1, MMP-9, Collagen I proteins. Each bar graph represents the mean ± SEM for three replicates (n = 3). Statistical significance was noted in comparison to the NC group (###*P* < 0.001, ##*P* < 0.01, #*P* < 0.05) and the UVB group (****P* < 0.001, ***P* < 0.01, **P* < 0.05).

Table 3. Effect of GrowGx™ combined with CP on mouse body weight.

Groups	Weight ($\bar{x} \pm s$, g)		
	First Week	Third Week	Sixth Week
NC	28.78 ± 1.37	39.07 ± 3.06	48.18 ± 4.53
UVB	27.98 ± 1.72	40.50 ± 2.29	48.47 ± 4.01
GrowGx™	27.95 ± 1.94	39.78 ± 3.77	48.15 ± 4.13
CP	29.22 ± 1.15	40.33 ± 3.23	48.05 ± 3.76
GrowGx™ + CP	28.83 ± 1.82	39.97 ± 2.77	48.88 ± 5.49
VC	29.17 ± 1.10	40.47 ± 2.30	49.43 ± 3.37

Table 4. Effect of GrowGx™ combined with CP on organ index in mice.

Groups	Organ Index ($\bar{x} \pm s$, mg/g)		
	Liver	Spleen	Thymus
NC	52.85 ± 5.87	3.06 ± 0.25	0.76 ± 0.12
UVB	52.14 ± 6.61	3.33 ± 0.61	0.71 ± 0.18
GrowGx™	51.07 ± 5.06	3.36 ± 0.50	0.69 ± 0.11
CP	54.12 ± 8.66	3.17 ± 0.35	0.72 ± 0.154
GrowGx™ + CP	54.51 ± 11.21	3.14 ± 0.60	0.67 ± 0.13
VC	52.65 ± 7.91	3.19 ± 0.37	0.73 ± 0.12

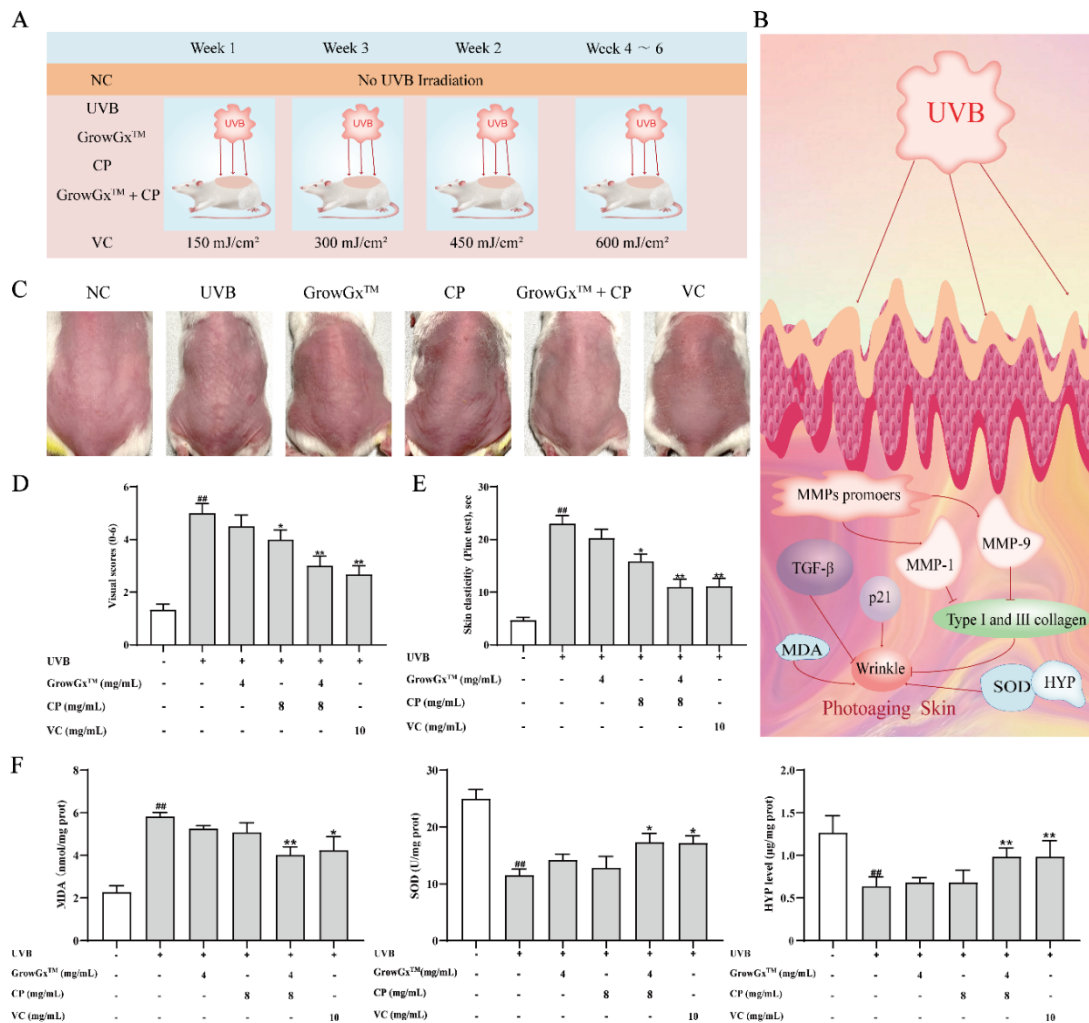


Figure 6. Macroscopic evaluation of mouse skin

(A) an experimental flowchart for the animal study, (B) a schematic diagram illustrating the mechanism of photoaging under investigation, (C) images of dorsal skin in mice at the end of week 6, (D) visual aging scores for the dorsal skin of mice at week 6, (E) elasticity recovery times for the dorsal skin of mice at week 6, and (F) levels of MDA, SOD, and HYP in the dorsal skin of mice at week 6. Each bar graph represents the mean \pm Standard Error of the Mean (SEM) based on six replicates ($n = 6$). (Note: Results show statistical significance compared to the NC group (^{###} $P < 0.001$, ^{##} $P < 0.01$, [#] $P < 0.05$) and the UVB group (^{***} $P < 0.001$, ^{**} $P < 0.01$, ^{*} $P < 0.05$).

levels ($P < 0.01$), indicative of a disrupted oxidative balance. Following treatment with GrowGx™ combined with CP, the oxidative balance in mouse skin was restored. These findings are in line with the cell experiments (Figure 3A), further validating that treatment with GrowGx™ combined with CP can restore SOD and HYP levels and suppress MDA content, thus achieving anti-aging effects.

9. Histopathological Assessment of Mouse Skin

In the NC group, the mouse skin epidermis appeared uniform, smooth, and intact (Figure 7A), with the dermis containing tightly packed and finely structured collagen fibers (Figure 7B). The UVB group demonstrated irregular thickening in both the epidermis and dermis ($P < 0.01$), attributed to irregular hyperproliferation of keratinocytes in the epidermis (Figure 7C) and degradation and disordered arrangement of dermal

collagen fibers (Figure 7D) (Peng et al., 2020). The CP group was effective in restoring dermal collagen ($P < 0.05$) but did not inhibit abnormal epidermal proliferation. However, the GrowGx™ combined with CP group normalized epidermal thickness ($P < 0.01$) and showed uniform distribution of dermal collagen fibers. These results suggest that GrowGx™ combined with CP can alleviate UV-induced skin aging.

10. Expression of p21, MMP-1, MMP-9, Collagen I, and TGF- β in Mouse Skin

Data indicate that by week 6, the UVB group exhibited significant increases in the expression of p21, MMP-1, and MMP-9 ($P < 0.01$), and significant decreases in Collagen I and TGF- β levels ($P < 0.01$). Conversely, the results for the GrowGx™ combined with CP group were opposite, consistent with the findings in Figures 8A and B.

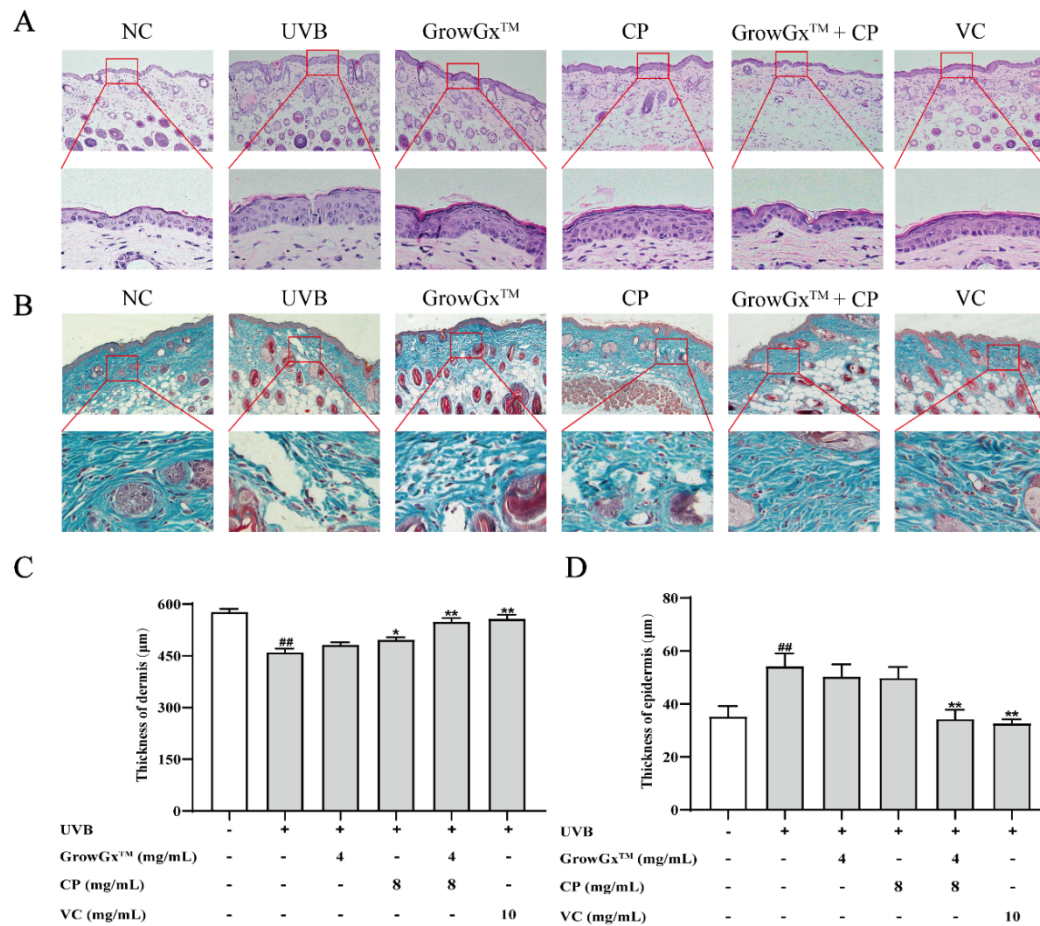


Figure 7. Histopathological assessment of mouse skin

(A) H&E staining of mouse skin, (B) Masson's trichrome staining of mouse skin, (C) Dermis thickness, and (D) Epidermis thickness in mice. Each bar graph represents mean \pm SEM for six replicates ($n = 6$) (Note: Results are statistically significant compared to the NC group ($###P < 0.001$, $##P < 0.01$, $*P < 0.05$) and the UVB group ($***P < 0.001$, $**P < 0.01$, $*P < 0.05$)).

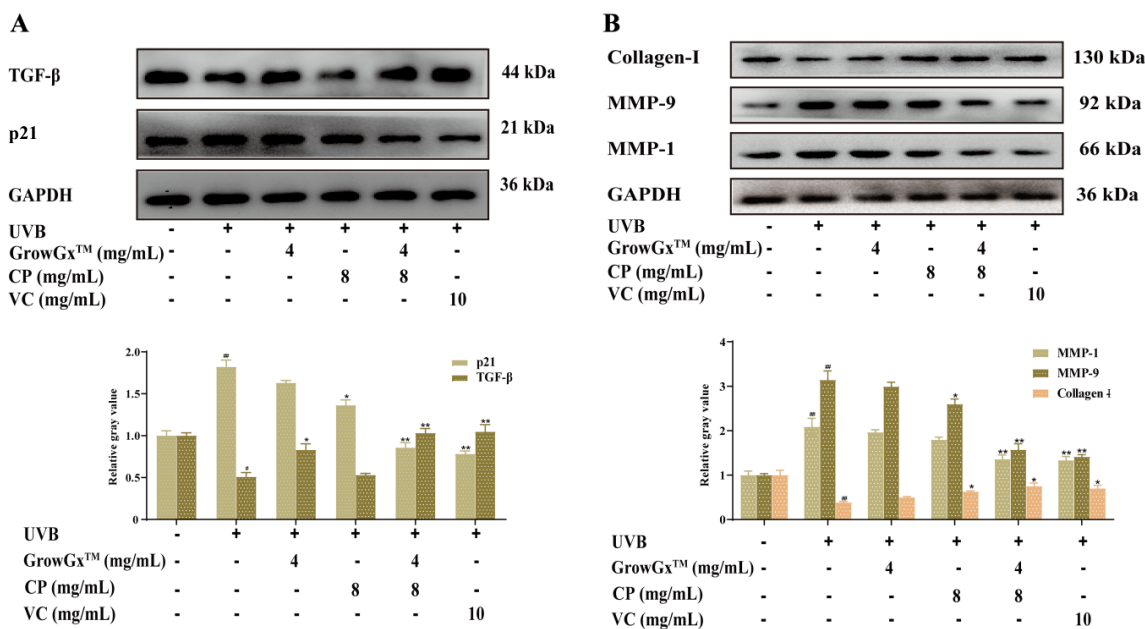


Figure 8. The levels of p21, MMP-1, MMP-9, Collagen I, and TGF- β in the dorsal skin of mice

(A) Expression of p21 and TGF- β proteins. (B) Expression of MMP-1, MMP-9, and Collagen I proteins. Each bar graph represents mean \pm SEM for three replicates ($n = 3$) (Note: Results are statistically significant compared to the NC group ($###P < 0.001$, $##P < 0.01$, $*P < 0.05$) and the UVB group ($***P < 0.001$, $**P < 0.01$, $*P < 0.05$)).

Discussion

The growing prevalence of global population aging, with an estimated one-quarter of the world's population being elderly by the mid-21st century (Xu et al., 2019), highlights the urgency in addressing age-related concerns. With improved living standards, there is an increasing demand for maintaining youthful skin appearances, which stands in contrast to the inevitable nature of skin aging. Consequently, mitigating skin aging has emerged as a focal point of contemporary research (Kerr et al., 2021). Small molecule peptides and compounds, recognized for their pronounced effectiveness and skin permeability, have become hotspots in cosmeceutical research (Kim et al., 2022; Zhang et al., 2022). This study delved into the anti-photoaging effects and mechanisms of the yeast fermentate GrowGx™ in conjunction with small molecule peptide CP, both in vitro and in vivo.

Previous laboratory studies have demonstrated that GrowGx™ at a concentration of 5 mg/mL significantly enhances fibroblast proliferation ($P < 0.05$) (Zhang et al., 2022). Our current findings reveal that at a concentration of 90 µg/mL, GrowGx™ can significantly promote the proliferation and migration of HaCaT cells ($P < 0.05$). Moreover, the combination of GrowGx™ (90 µg/mL) and CP (80 µg/mL) shows an even more pronounced effect in enhancing HaCaT cell proliferation and migration ($P < 0.01$). This enhanced efficacy is likely attributed to differences in cellular structures and sensitivities to the compounds, with HaCaT cells being more responsive to GrowGx™ at lower concentrations.

The combination of GrowGx™ and CP was found to restore the viability of UV-irradiated HaCaT cells and reduce intracellular SA-β-gal content, suggesting its potential in counteracting skin photoaging. Further investigation through cell scratch assays and measurements of MDA, SOD, and HYP levels indicates that the anti-photoaging properties of GrowGx™ combined with CP may be attributed to enhanced cell proliferation and restored cellular oxidative balance.

The safety and non-toxicity of cosmeceuticals are crucial for their acceptance and usage (Alves et al., 2020). In vivo studies indicate that GrowGx™ combined with CP does not elicit significant allergic or irritant reactions on mouse dorsal skin. Organ index measurements post-treatment reveal no significant toxicological effects, underscoring the safety and harmlessness of GrowGx™ combined with CP when applied to mouse skin. After six weeks of UVB exposure, the skin of the UVB group mice exhibited dryness, wrinkles, and reduced elasticity. Conversely, the skin of mice treated with GrowGx™ combined with CP displayed noticeable reductions in wrinkles and improvements in smoothness and refinement. Histological examination revealed that UVB exposure resulted in abnormal epidermal thickening and dermal collagen fiber degradation

in UVB group mice. In contrast, treatment with GrowGx™ combined with CP led to a restoration of skin tissue structure and an increase in collagen density, suggesting that GrowGx™ combined with CP is a promising cosmeceutical ingredient. Analysis of MDA, SOD, and HYP levels in mouse skin tissues showed trends consistent with those observed in HaCaT cells, further validating the efficacy of GrowGx™ combined with CP in restoring oxidative balance and promoting collagen synthesis both in vitro and in vivo.

p21, known to inhibit cyclin-dependent kinase (CDK) activity and regulate the cell cycle, shows increased expression during cellular aging (Hernandez-Segura et al., 2018). UVB irradiation induces MMP-1 secretion in HaCaT cells, which degrades Type I and III collagens. Type I collagen is the most abundant collagen subtype in skin connective tissue, followed by Type III (Wang et al., 2014; Pittayapruek et al., 2016). MMP-9 further breaks down collagen degraded by MMP-1 into fragments, leading to skin connective tissue collapse, wrinkle formation, or edema (Jung et al., 2010). Thus, our study found that in the UVB group, there was an increase in the expression of p21, MMP-1, and MMP-9, and a decrease in Collagen I and TGF-β, resulting in pronounced wrinkling. These findings align with previous literature (Jung et al., 2010). The GrowGx™ combined with CP group exhibited a significant reduction in wrinkles, decreased expression of p21, MMP-1, and MMP-9, and increased expression of Collagen I and TGF-β, suggesting that GrowGx™ combined with CP can inhibit UVB-induced skin photoaging.

In summary, GrowGx™ combined with CP attenuates photoaging by downregulating p21, MMP-1, and MMP-9 expression, and upregulating Collagen I and TGF-β expression. It promotes cell proliferation and restores oxidative balance, thereby counteracting skin photoaging.

Abbreviations

CP, Collagen Peptide; UVB, Ultraviolet B; SA-β-gal, Senescence-Associated β-Galactosidase; MDA, Malondialdehyde; SOD, Superoxide Dismutase; HYP, Hydroxyproline; VC, Vitamin C; ROS, Reactive Oxygen Species; MMPs, Matrix Metalloproteinases; MMP-1, Matrix Metalloproteinase-1; MMP-9, Matrix Metalloproteinase-9; Collagen I, Type I Collagen; p21, Waf1/Cip1; TGF-β, Transforming Growth Factor Beta; MED, Minimal Erythema Dose.

Declarations

Ethics Approval and Consent to Participate: Applicable.

Consent for Publication: Not applicable.

Availability of Data and Materials: The datasets and reagents

used in this study are available upon reasonable request from the corresponding author.

Conflict of Interest

The authors declare no competing interests.

Funding

This work was supported by the Guangxi Major Science and Technology Project: Research on Synergistic Tackling and Quality Improvement of Guangxi Traditional Chinese Medicine and Ethnic Medicine Industrial Cluster (Guike AA23023035).

Authors' Contributions: Xiaoqun Duan conceptualized and directed the study. Zhijia Lu performed the experiments, collected, and analyzed the data. Zhijia Lu and Meng Liu contributed to the study design and further drafting. Xi Lu revised the manuscript. All authors have read and approved the final manuscript.

References

- [1] Alves A, Sousa E, Kijjoo A, Pinto M. Marine-derived compounds with potential use as cosmeceuticals and nutricosmetics. *Molecules*. 2020;25(11):2536.
- [2] Bang E, Kim DH, Chung HY. Protease-activated receptor 2 induces ROS-mediated inflammation through Akt-mediated NF-kappaB and FoxO6 modulation during skin photoaging. *Redox Biol*. 2021;44:102022.
- [3] Battie C, Jitsukawa S, Bernerd F, Bion SD, Marionnet, C, Verschoore M. New insights in photoaging, UVA induced damage and skin types. *Exp Dermatol*. 2014;23 Suppl 1: 7-12.
- [4] Bolke L, Schlippe G, Gerss J, Voss W. A collagen supplement improves skin hydration, elasticity, roughness, and density: results of a randomized, placebo-controlled, blind study. *Nutrients*. 2019;11(10): 2494.
- [5] Cao C, Xiao Z, Tong H, Liu Y, Wu Y, Ge C. Oral intake of chicken bone collagen peptides anti-skin aging in mice by regulating collagen degradation and synthesis, inhibiting inflammation and activating lysosomes. *Nutrients*. 2022;14(8): 1622.
- [6] Chen S, He Z, Xu J. Application of adipose-derived stem cells in photoaging: basic science and literature review. *Stem Cell Res Ther*. 2020;11(1): 491.
- [7] Choi SI, Han HS, Kim JM, Park G, Jang YP, Shin YK, Ahn HS, Lee SH, Lee KT. Eisenia bicyclis extract repairs UVB-induced skin photoaging in vitro and in vivo: photoprotective effects. *Mar Drugs*. 2021;19(12): 693.
- [8] Cicek D, Demir B, Orhan C, Tuzcu M, Ozercan IH, Sahin H, Komorowski J, Ojalvo SP, Sylla S, Sahin K. The protective effects of a combination of an arginine silicate complex and magnesium biotinate against UV-induced skin damage in rats. *Front Pharmacol*. 2021;12: 657207.
- [9] Gilchrist BA. A review of skin ageing and its medical therapy. *Br J Dermatol*. 1996;135(6): 867-75.
- [10] Han HS, Shin JS, Myung DB, Ahn HS, Lee SH, Kim HJ, Lee HJ. Hydrangea serrata (Thunb.) Ser. extract attenuate UVB-induced photoaging through MAPK/AP-1 inactivation in human skin fibroblasts and hairless mice. *Nutrients*. 2019;11(3): 533.
- [11] Hernandez-Segura A, Nehem J, Demaria M. Hallmarks of cellular senescence. *Trends Cell Biol*. 2018;28(6): 436-53.
- [12] Im AR, Ji KY, Park IW, Lee JY, Kim KM, Na MK, Chae S. Anti-photoaging effects of four insect extracts by downregulating matrix metalloproteinase expression via mitogen-activated protein kinase-dependent signaling. *Nutrients*. 2019;11(5): 1159.
- [13] Im AR, Park IW, Ji KY, Lee JY, Kim KM, Na MK, Chae S. Protective effects of *Oxya chinensis sinuosa* Mishchenko against ultraviolet B-induced photodamage in hairless mice. *BMC Complement Altern Med*. 2019;19(1): 286.
- [14] Jiang H, Zhou X, Chen L. Asiaticoside delays senescence and attenuate generation of ROS in UV-exposure cells through regulates TGF-beta1/Smad pathway. *Exp Ther Med*. 2022;24(5): 667.
- [15] Jung SK, Lee KW, Kim HY, Oh MH, Byun S, Lim SH, Heo YS, Kang NJ, Bode AM, Dong Z, Lee HJ. Myricetin suppresses UVB-induced wrinkle formation and MMP-9 expression by inhibiting Raf. *Biochem Pharmacol*. 2010;79(10): 1455-61.
- [16] Kerr CL. Geroscience approaches to women's health in an aging world. *J Gerontol A Biol Sci Med Sci*. 2021;76(9): 1531-32.
- [17] Kim J, Lee SG, Lee J, Choi S, Suk J, Lee JH, Yang JH, Yang JS, Kim J. Oral supplementation of low-molecular-weight collagen peptides reduces skin wrinkles and improves biophysical properties of skin: a randomized, double-blinded, placebo-controlled study. *J Med Food*. 2022;25(12): 1146-54.
- [18] Lopez-Otin C, Blasco M A, Partridge L, Serrano M, Kroemer G. The hallmarks of aging. *Cell*. 2013;153(6): 1194-217.
- [19] Lopez-Otin C, Blasco MA, Partridge L, Serrano M, Kroemer G. Hallmarks of aging: An expanding universe. *Cell*. 2023;186(2): 243-78.
- [20] Mu J, Ma H, Chen H, Zhang XX, Ye MY. Luteolin prevents UVB-induced skin photoaging damage by modulating SIRT3/ROS/MAPK signalling: An in vitro and in vivo studies. *Front Pharmacol*. 2021;12: 728261.
- [21] Peng Z, Chen B, Zheng Q, Zhu G, Cao W, Qin X, Zhang C. Ameliorative effects of peptides from the Oyster (*Crassostrea hongkongensis*) protein hydrolysates against UVB-induced skin photodamage in mice. *Mar Drugs*. 2020;18(6): 288.
- [22] Pittayapruek P, Meephansan J, Prapapan O, Komine M, Ohtsuki M. Role of matrix metalloproteinases in photoaging and photocarcinogenesis. *Int J Mol Sci*. 2016;17(6):868.
- [23] Song H, Zhang L, Luo Y, Zhang S, Li B. Effects of collagen peptides intake on skin ageing and platelet release in chronologically aged mice revealed by cytokine array analysis. *J Cell Mol Med*. 2018;22(1): 277-88.
- [24] Song H, Zhang S, Zhang L, Li B. Effect of orally administered collagen peptides from bovine bone on skin aging in chronologically aged mice. *Nutrients*. 2017;9(11): 1209.
- [25] Subedi L, Lee TH, Wahedi HM, Baek SH, Kim SY. Resveratrol-enriched rice attenuates UVB-ROS-induced skin aging via downregulation of inflammatory cascades. *Oxid Med Cell Longev*. 2017;2017: 8379539.
- [26] Tian L, Ke D, Hong Y, Zhang C, Tian D, Chen L, Zhan L, Zong S. Artesunate treatment ameliorates ultraviolet irradiation-driven skin photoaging via increasing beta-catenin expression. *Aging (Albany NY)*. 2021;13(23): 25325-41.
- [27] Vats K, Kruglov O, Mizes A, Samovich SN, Amoscato AA, Tyurin

- VA, Tyurina YY, Kagan VE, Bunimovich YL. Keratinocyte death by ferroptosis initiates skin inflammation after UVB exposure. *Redox Biol.* 2021;47: 102143.
- [28] Wang L, Wang Q, Qian J, Liang Q, Wang Z, Xu J, He S, Ma H. Bioavailability and bioavailable forms of collagen after oral administration to rats. *J Agric Food Chem.* 2015;63(14): 3752-6.
- [29] Wang Y, Chem H, Wang W, Wang R, Liu ZL, Zhu, W, Lian S. N-terminal 5-mer peptide analog P165 of amyloid precursor protein inhibits UVA-induced MMP-1 expression by suppressing the MAPK pathway in human dermal fibroblasts. *Eur J Pharmacol.* 2014;734: 1-8.
- [30] Xu K, Guo Y, Li Z, Wang Z. Aging biomarkers and novel targets for anti-aging interventions. *Adv Exp Med Biol.* 2019;1178: 39-56.
- [31] Yue Q, Chen X, Gao J, Gong Q, Shi J, Li F. Dendrobine protects HACAT cells from H₂O₂-induced oxidative stress and apoptosis damage via Nrf2/Keap1/ARE signaling pathway. *Toxicol Appl Pharmacol.* 2022;454: 116217.
- [32] Zhang C, Lv J, Qin X, Peng Z, Lin H. Novel antioxidant peptides from *Crassostrea hongkongensis* improve photo-oxidation in UV-induced HaCaT Cells. *Mar Drugs.* 2022;20(2): 100.
- [33] Zhang H, Wan J, Zhao Y, Wu Y, Lei X, Duan X. Mechanism and clinical observation of effect of GrowGx™ yeast fermentation product extract on photo-aged HFF-1 cells. *J Medicinal Plant.* 2022;13(1): 26-9.
- [34] Zhang L, Zhang S, Song H, Li B. Ingestion of collagen hydrolysates alleviates skin chronological aging in an aged mouse model by increasing collagen synthesis. *Food Funct.* 2020;11(6): 5573-80.
- [35] Zhang XD, Wu HY, Wu D, Wang YY, Chang JH, Zhai ZB, Meng AM, Liu PX, Zhang AL, Fan FY. Toxicologic effects of gold nanoparticles in vivo by different administration routes. *Int J Nanome.* 2010;5: 771-81.